DMD Fast Forward. Published on August 30, 2010 as doi:10.1124/dmd.110.035006

DMD #35006

DIVERSITY IN ANTIOXIDANT RESPONSE ENZYMES IN PROGRESSIVE STAGES OF HUMAN NON-ALCOHOLIC FATTY LIVER DISEASE

Rhiannon N. Hardwick, Craig D. Fisher, Mark J. Canet, April D. Lake, Nathan J. Cherrington

Department of Pharmacology and Toxicology, University of Arizona, Tucson AZ, USA

DMD Fast Forward. Published on August 30, 2010 as DOI: 10.1124/dmd.110.035006
This article has not been copyedited and formatted. The final version may differ from this version.

Running Title: Changes in ARE enzymes in non-alcoholic fatty liver disease

Corresponding author: Nathan J. Cherrington
1703 E Mabel St
Tucson AZ 85721
PH: (520) 626-0219
Fax: (520) 626-2466
cherrington@pharmacy.arizona.edu

Text pages: 26

Figures: 6

References: 37

Words in Abstract: 250

Words in Introduction: 726

Words in Discussion: 1,494

Abbreviations: NAFLD, non-alcoholic fatty liver disease; NASH, non-alcoholic steatohepatitis; NQO1, NAD(P)H:quinone oxidoreductase 1; GST, glutathione S-transferase; GCL, glutamate cysteine ligase; GCLC, glutamate cysteine ligase catalytic subunit; GCLM, glutamate cysteine ligase modifier subunit; GSH, reduced glutathione; GSSG, oxidized glutathione; DCPIP, 2,6-Dichlorophenol indophenol; CDNB, 1-Chloro-2,4-dinitrobenzene; HNE, 4-hydroxy-2-nonenal; MDA, malondialdehyde

DMD Fast Forward. Published on August 30, 2010 as DOI: 10.1124/dmd.110.035006
This article has not been copyedited and formatted. The final version may differ from this version.

Abstract

Non-alcoholic fatty liver disease (NAFLD), which occurs in approximately 17-40% of Americans, encompasses progressive stages of liver damage ranging from steatosis to non-alcoholic steatohepatitis (NASH). Inflammation and oxidative stress are known characteristics of NAFLD; however the precise mechanisms occurring during disease progression remain unclear. The purpose of the current study was to determine whether the expression or function of enzymes involved in the antioxidant response—NAD(P)H:quinone oxidoreductase 1, glutathione *S*-transferase, glutamate cysteine ligase—are altered in the progression of human NAFLD. Human livers staged as normal, steatotic, NASH (fatty) and NASH (not fatty) were obtained from the Liver Tissue Cell Distribution System. NQO1 mRNA, protein, and activity tended to increase with disease progression. mRNA levels of the GST isoforms A1, A2, A4, M3, and P1 increased with NAFLD progression. Similarly, GST A and P protein increased with progression; however GST M protein levels tended to decrease. Interestingly, total GST activity toward the substrate CDNB decreased with NAFLD progression. GSH synthesis does not appear to be significantly dysregulated in NAFLD progression; however, the GSH:GSSG redox ratio appeared to be reduced with disease severity, indicating the presence of oxidative stress and depletion of GSH throughout progression of NAFLD. MDA concentrations were significantly increased with disease progression, further indicating the presence of oxidative stress. Nuclear immunohistochemical staining of Nrf2, an indicator of activation of the transcription factor, was evident in all stages of NAFLD. The current data suggest that Nrf2 activation occurs in response to disease progression followed by induction of specific Nrf2 targets, while functionality of specific antioxidant defense enzymes appear to be impaired as NAFLD progresses.

Introduction

Non-alcoholic fatty liver disease (NAFLD) is recognized as an epidemic of modern, industrialized countries. Reports estimate that approximately 17-40% of the United States population is affected by NAFLD (Ali *et al.*, 2009;McCullough, 2006). It is a complex disease consisting of various stages characterized by progressive levels of hepatocellular damage. NAFLD originates as an infiltration of triglycerides within hepatocytes (Angulo, 2002) known as simple fatty liver (steatosis). Steatosis is generally considered a benign condition, though it renders the liver susceptible to further damage (Marra *et al.*, 2008;Adams *et al.*, 2007). The initial accumulation of lipids within hepatocytes is described as the "first hit" in NAFLD pathogenesis, and is believed to be associated with increased sensitivity to oxidative stress (Nagata *et al.*, 2007). Steatosis can progress to the more severe non-alcoholic steatohepatitis (NASH) which is associated with an increase in inflammation, fibrosis, oxidative stress and more widespread damage (Marra *et al.*, 2008;Kleiner *et al.*, 2005).

Though the mechanisms are not entirely clear, the presentation of oxidative stress is regarded as the "second hit" in NAFLD pathogenesis (Nagata *et al.*, 2007). Additionally, the development of inflammation and fibrosis, which cause impairments in liver function, are important factors in the differentiation of steatosis from NASH (Marra *et al.*, 2008). Furthermore, activation of inflammatory cells and mitochondrial dysfunction are believed to be significant contributors to the perpetuation of reactive oxygen species (ROS) production in the progression from steatosis to NASH (Marra *et al.*, 2008). NASH, which is considered to be the end-stage of NAFLD, is estimated to affect 5.7-17% of the United States population, and can further progress to cirrhosis and liver failure (McCullough, 2006). Approximately 15-25% of NASH patients are estimated to progress to cirrhosis with 30-40% eventually surrendering to liver disease-associated deaths (McCullough, 2006).

Oxidative stress is a cellular state in which the generation of such harmful molecules as ROS, peroxidized lipids, reactive quinones, and electrophiles is disproportionate to the cell's ability to remove these destructive agents. The capacity of a cell to manage oxidative stress is primarily mediated through antioxidant response elements (ARE), which are largely under the control of the transcription factor NF-E2-related nuclear factor 2 (Nrf2) (Jaiswal, 2004;Itoh *et al.*, 1997). Nrf2 is primarily a cytosolic protein due to proteasomal degradation regulated by Keap1 (Zhang, 2006;Jaiswal, 2004). When a cell is undergoing oxidative stress, Nrf2 escapes Keap1-mediated degradation, translocates to the nucleus, binds to ARE sequences within the promoters of target genes, and induces expression of Phase I and II metabolizing enzymes and transporters pivotal to the maintenance of oxidative stress-inducing molecules (Jaiswal, 2004;Nakata *et al.*, 2006;Zhang, 2006). Such enzymes include NAD(P)H:quinone oxidoreductase-1 (NQO1), glutathione S-transferase isoforms (GSTs), and glutamate cysteine ligase (GCL) subunits (Itoh *et al.*, 1997;Nguyen *et al.*, 2000;Nakata *et al.*, 2006).

NQO1 is a cytosolic protein that catalyzes the two electron reduction of reactive quinones which are capable of producing ROS and initiating redox cycling (Ross *et al.*, 2004;Talalay *et al.*, 2004;Jaiswal, 2000). Human GSTs are a large family of detoxifying enzymes that catalyze the conjugation of GSH to reactive electrophiles (Hayes *et al.*, 2005). GSTs can be found in the cytosol, mitochondria, and microsomal membranes of most tissues throughout the body (Hayes *et al.*, 2005). The cytosolic GST isoforms consist of several families, some of which are included in the alpha, mu, and pi classes—each of which have multiple members (Hayes *et al.*, 2005;Pastore *et al.*, 2003). The alpha and mu classes have received significant attention as Nrf2 target genes, and specific alpha isoforms are important for the inactivation of oxidative stress-inducing lipid peroxides. GCL is the rate-limiting step in the synthesis of GSH, and is composed of two subunits, catalytic (GCLC) and modifier (GCLM) (Lu, 2008). As a cofactor for

GST isoforms, disruptions in GSH synthesis have the potential to severely disturb the detoxifying capacity of hepatic GSTs. However, reductions in GSH concentration do not always correlate with GCL expression or activity, such as during periods of significant depletion of GSH pools (Lu, 2008;Pastore *et al.*, 2003).

Due to the increasing prevalence of NAFLD, elucidating the mechanisms of oxidative stress-induced injury within the liver is vital to understanding the pathogenesis of NAFLD and susceptibility to further damage. The focus of the current study was to evaluate the expression and activity of NQO1, GST isoforms, and GSH synthesis in the livers of adult patients diagnosed with the progressive stages of NAFLD.

DMD Fast Forward. Published on August 30, 2010 as DOI: 10.1124/dmd.110.035006
This article has not been copyedited and formatted. The final version may differ from this version.

Materials and Methods

Materials. Tris-HCl, EDTA, KCl, phenylmethanesulphonyl fluoride (PMSF), 2,6-Dichlorophenol-indophenol (DCPIP), NAD(P)H, 1-Chloro-2,4-dinitrobenzene (CDNB), glutathione (GSH), diaminobenzidine tetrahydrochloride (DAB), and H_2O_2 were obtained from Sigma-Aldrich (St. Louis, MO).

Human Liver Samples and Tissue Preparations. Frozen and formalin-fixed, paraffin-embedded adult human liver tissue was obtained from the Liver Tissue Cell Distribution System at the University of Minnesota, Virginia Commonwealth University and the University of Pittsburgh. All samples were scored and categorized by a medical pathologist at the Liver Tissue Cell Distribution System according to the NAFLD Activity Score system developed by Kleiner, et al. as part of the service provided by the agency to NIH-funded investigators (Kleiner *et al.*, 2005). Diagnosis was later confirmed by histological examination at the University of Arizona. Donor information, including age and gender, has been published previously (Fisher *et al.*, 2009). The samples were diagnosed as normal (n=20), steatotic (n=12), NASH with fatty liver (NASH fatty, n=11), and NASH without fatty liver (NASH not fatty, n=11). Samples exhibiting >10% fatty infiltration of hepatocytes were considered steatotic. NASH (fatty) samples were diagnosed based upon >5% fatty infiltration of hepatocytes with significant inflammation and fibrosis. NASH (not fatty) samples were differentiated from NASH (fatty) samples by a reduction in fatty deposits within the hepatocytes (<5%). Furthermore, NASH (not fatty) samples presented more marked inflammation and fibrotic branching. Total RNA was isolated from human liver tissue using RNAzol B reagent (Tel-Test Inc., Friendswood, TX) according to the manufacturer's recommendations. RNA concentrations were determined by UV spectrophotometry. Integrity of the RNA was confirmed by ethidium bromide staining following agarose gel electrophoresis. Cytosolic fractions of human liver tissue were prepared by homogenization in buffer containing

50 mM Tris-HCl (pH 7.4), 1 mM EDTA and 154 mM KCl with 0.5 mL/100 mL 100 mM PMSF at 4°C. Homogenates were centrifuged at 10,000 x g for 30 minutes and the supernatant was transferred to clean microcentrifuge tubes. Samples were then centrifuged at 100,000 x g for 70 minutes and the supernatant was retained as the cytosolic fraction. Protein concentrations were determined using the Pierce BCA Protein Quantitation Assay (Thermo Scientific, Rockford, IL) per the manufacturer's protocol.

Branched DNA Assay. Specific oligonucleotide probes (see Supplemental Data Table 1) for NQO1, GCLC, and GCLM were diluted in lysis buffer supplied by the Quantigene™ HV Signal Amplification Kit (Genospectra, Fremont, CA). Substrate solution, lysis buffer, capture hybridization buffer, amplifier and label probe buffer used in the analysis were all obtained from the Quantigene Discovery Kit (Genospectra, Fremont, CA). The assay was performed in a 96-well plate in which total RNA (1 µg/µl; 10 µl) was added to the capture hybridization buffer with 50 µl of the diluted probe set. The total RNA was then allowed to hybridize to the probe set overnight at 53°C. Hybridization steps were performed the following day per the manufacturer's protocol. Luminescence of the samples was measured with a Quantiplex™ 320 bDNA luminometer interfaced with Quantiplex™ Data Management Software Version 5.02.

Real-Time Reverse Transcriptase Polymerase Chain Reaction (qPCR). cDNA was reverse-transcribed from total RNA using the Transcriptor First Strand cDNA Synthesis Kit (Roche, Indianapolis IN) per the manufacturer's protocol. Specific primers for GST isoforms A1, A2, A4, M1, M2, M3, M4 and P1 (see Appendix B) were synthesized by Integrated DNA Technologies (Coralville, IA). Reactions were performed using the LightCycler 480 Probes Master Kit (Roche, Indianapolis IN) and Universal ProbeLibrary Probes (Roche, Indianapolis IN) according to the manufacturer's protocol. Briefly, the reaction was performed as follows: one denaturation cycle

(95°C for 2 minutes), 45 amplification cycles (95°C for 10 seconds, 60°C for 30 seconds) and one cooling period (40°C for 30 seconds). Relative mRNA levels were normalized to GAPDH.

NQO1 Activity assay. NQO1 activity was determined by measuring the colorimetric reduction of DCPIP at 600 nm for an interval of one minute as previously described (Aleksunes *et al.*, 2006a). The reaction was performed in triplicate in a 1mL format containing 200 μM NAD(P)H, 40 μM DCPIP and liver cytosol in a Tris-HCl buffer (25 mM Tris pH 7.4, 0.7 mg/mL bovine serum albumin). Similarly, inhibition reactions were performed with the addition of 20μM Dicumarol to the reaction mixture. The activity was determined by the difference in absorbance rates of the uninhibited and inhibited reaction rates, and was then normalized to total cytosolic protein content.

GST Activity Assay. GST activity was quantified by spectrophotometry according to established methods using 1-Chloro-2,4-dinitrobenzene (CDNB) which is a substrate for the GST isoforms A1, A2, A4, M1, M2, M3, M4 and P1 (Current Protocols in Toxicology, 1999). Specifically, 1 mL reactions of 1 mM CDNB (prepared in 95% ethanol), 1 mM GSH, 0.1 M Sodium phosphate buffer (pH 6.5) and liver cytosol were measured at 340 nm for a period of one minute. All reactions were performed in triplicate. Enzyme activity was calculated as the difference of the rate of a sample reaction from a simultaneous blank reaction devoid of liver cytosol, and was normalized to total cytosolic protein content.

Immunoblot Protein Analysis. Cytosolic proteins (20μg/well) were separated by SDS-PAGE and transferred to PVDF membranes. The following mouse monoclonal antibodies were obtained from Abcam, Inc. (Cambridge, MA): 1:1000 NQO1 (A180), 1:500 GSTA, 1:500 GSTP (3F2C2). GCL protein was detected using mouse monoclonal antibodies from Abnova (Taipei City, Taiwan): 1:8000 GCLC (3H1) and 1:3000 GCLM (2B8). Levels of GSTM (1:3000, Abcam, Inc.,

Cambridge, MA) and total ERK (1:1000 C-16 and C-14, Santa Cruz Biotechnology, Inc., Santa Cruz, CA) were measured using goat polyclonal antibodies. Quantification of relative protein expression was determined using image processing and analysis with Image J software (NIH, Bethesda, MD) and normalized to total ERK.

Glutathione Assay. Glutathione (GSH) concentrations were determined using the BioVision Glutathione Assay Kit (Mountain View, CA) per the manufacturer's recommendations in a 96-well format. Briefly, ~40 mg of tissue was homogenized and preserved with GSH buffer and 6 N perchloric acid. Samples were then precipitated with 3 N potassium hydroxide and centrifuged for 2 minutes at 13,000 x g. To detect reduced glutathione (GSH), 5 µl of the neutralized sample was incubated with o-phthalaldehyde probe (OPA) and GSH buffer for 40 minutes. To detect oxidized glutathione (GSSG), 1 µl of neutralized sample was incubated with GSH buffer and 10 µl of GSH quencher for 10 minutes, followed by reducing agent and OPA for 40 minutes. Fluorescence readings were captured using a SPECTRAmax GEMINI XS (Molecular Devices Corporation, Sunnyvale, CA) fluorescence reader.

Thiobarbituric Acid Reactive Substances (TBARS) Assay. Malondialdehyde (MDA) concentrations were determined using the Cayman Chemical TBARS Assay Kit (Ann Arbor, MI) per the manufacturer's recommendations for colorimetric measurement of MDA. Briefly, ~25 mg of tissue was sonicated on ice in RIPA lysis buffer containing 1% NP-40, 1% w/v sodium deoxycholate, 0.1% SDS, 0.15 M NaCl, 0.01 M sodium phosphate pH 8.0, 2 mM EDTA, and 1 Protease Inihibitor Cocktail Tablet per 25 mL (Roche, Indianapolis, IN). Samples were then centrifuged at 1,600 x g for 10 minutes at 4°C and the supernatant preserved for analysis. To 100 µL of each sample and standard curve solutions, 100 µL of provided SDS solution was added followed by 4 mL of color reagent. Samples and standard curve solutions were boiled for 1 hour and the reaction was terminated by incubation on ice for 10 minutes followed by

DMD Fast Forward. Published on August 30, 2010 as DOI: 10.1124/dmd.110.035006
This article has not been copyedited and formatted. The final version may differ from this version.

centrifugation at 1,600 x g for 10 minutes at 4°C. 150 µL of samples and standard curve solutions were loaded in duplicate onto a 96 well plate and absorbance read at 540 nm in a BioTek Powerwave HT (Winooski, VT) spectrophotometer.

Immunohistochemistry (IHC). Immunohistochemical staining for Nrf2 was performed on formalin-fixed paraffin-embedded human liver samples. Briefly, tissue sections were de-paraffinized in xylene and re-hydrated in ethanol, followed by antigen retrieval in citrate buffer (pH 6.0). Endogenous peroxidase activity was blocked with 0.3% (v/v) H_2O_2 in methanol for 20 minutes. All samples were incubated with a 1:75 solution of Nrf2 (C-20) antibody (Santa Cruz Biotechnology, Santa Cruz CA) overnight at 4°C. Antibody binding was detected with biotinylated goat anti-rabbit IgG (Vector Laboratories, Burlingame CA) and an avidin-biotin complex (Vector Laboratories, Burlingame CA). Color development was performed with a solution of 0.5% 3,3'-diaminobenzidine tetrahydrochloride (DAB) in 0.015% H_2O_2 (0.01M phosphate-buffered saline, pH 7.2). All slides were imaged with a Nikon Eclipse E4000 microscope and a Sony Exwave DXC-390 camera.

Quantification of Nrf2 Nuclear Translocation. Hepatocyte nuclei positive for Nrf2 staining and hepatocyte nuclei negative for Nrf2 staining were quantified within a 20X field of vision with a total of ten fields assessed for each sample. The number of total hepatocytes was calculated from the positive and negative nuclei counts, and was used to determine the percentage of positive nuclei within a field. The average number of positive nuclei, negative nuclei, total nuclei and percent positive nuclei was assessed for each diagnostic category.

Statistical Analysis. The samples within this study can be categorized by disease progression/severity: normal<steatosis<NASH (fatty)<NASH (not fatty). All data collected in this study were continuous outcomes, but exhibited a skewed distribution. Therefore, median values

rather than mean were compared and the results presented as box-and-whisker plots. Data were analyzed by a non-parametric trend analysis with a significance level of $p \leq 0.05$ to determine significant increases or decreases with disease progression/severity. All analyses were performed with Stata10 software (Stata, College Station, TX).

Results

Human NAFLD Histology. Representative images of hematoxylin and eosin (H&E) staining of human liver samples staged as normal, steatotic, NASH (fatty) and NASH (not fatty) are shown in Figure 1. A diagnosis of steatosis was made for samples exhibiting >10% fatty infiltration of hepatocytes. Samples exhibiting >5% fatty infiltration of hepatocytes with significant inflammation and fibrosis were staged as NASH (fatty). Those samples presenting with a reduction in fatty deposits within the hepatocytes to <5% with increased inflammation and branching fibrosis were diagnosed as NASH (not fatty). Microvesicular lipid deposits are readily apparent in the steatotic samples, and sinusoidal structure remains somewhat intact. The NASH (fatty) stage is characterized by macrovesicular fatty deposits within hepatocytes and the development of inflammation and fibrosis. As the liver progresses from NASH (fatty) to NASH (not fatty), the infiltration of fatty deposits is greatly reduced; however inflammation increases, as does fibrosis.

NQO1 Expression and Activity in Human NAFLD Progression. Gene expression of antioxidant response enzymes is indicative of Nrf2 transcriptional activation of the ARE. NQO1 gene expression was measured in human liver samples by assessing the levels of NQO1 mRNA using the bDNA assay, shown in Figure 2A. There was an increasing trend in NQO1 mRNA expression with progression of NAFLD. An immunoblot analysis of NQO1 protein levels in human cytosolic liver samples was conducted and normalized to Total ERK. Representative immunoblots with two samples from each diagnostic category and densitometry results of NQO1 in each stage of NAFLD are shown in Figure 2B and 2A, respectively. Densitometric analysis of relative NQO1 protein levels in all 54 human liver samples revealed an increasing trend in NQO1 protein with disease progression. The enzymatic activity of NQO1 protein was

measured in human liver cytosolic samples using DCPIP as the substrate. Enzymatic activity of NQO1 was significantly increased with progression of NAFLD.

GST Isoform Expression and Pan-GST Activity in Human NAFLD Progression. The expression of various GST isoforms is also dependent upon the ARE, and thus, transcriptional activation by Nrf2. Due to significant homology among the GST isoforms, mRNA levels could not be measured by bDNA analysis which requires the use of multiple oligonucleotides to identify specific mRNA molecules. Therefore, relative mRNA levels of the GST isoforms A1, A2, A4, M1, M2, M3, M4, and P1 were measured by qPCR in each stage of NAFLD. Shown in Figure 3A, mRNA levels of the GST A4, A2, A4, M3, and P1 isoforms exhibited a significant increasing trend with disease progression. GST protein levels in cytosolic liver fractions were assessed for each isoform family (GSTA, GSTM, and GSTP), and normalized to Total ERK. Protein levels were measured for all 54 liver specimens in the study. Representative immunoblots depicting two samples from each diagnostic category and densitometry results are shown in Figure 3C and 3B, respectively. There were increasing trends in expression for both GST A and P protein. In contrast, GST M protein levels were decreased with NAFLD progression. The functional capability of the GST isoforms to effectively conjugate GSH to electrophilic substrates was determined spectrophotometrically in human liver cytosolic samples using CDNB as a pan-GST substrate. Shown in Figure 3D, a significant decreasing trend in GST enzymatic activity was observed with NAFLD progression.

GCL Expression. mRNA and protein levels of GCL, the rate-limiting enzyme in the synthesis of GSH, were assessed by the bDNA assay and immunoblot analysis in human liver samples. mRNA results of GCLC, the catalytic subunit of GCL, and GCLM, the modifier subunit, are shown in Figure 4A. No significant alterations were observed in the mRNA levels of GCLC; however, GCLM mRNA levels exhibited an increasing trend as NAFLD severity increased. The

densitometric results of GCLC and GCLM protein levels in all 54 human liver samples, along with representative immunoblots depicting two samples from each diagnostic category, are shown in Figure 4A and 4B, respectively. No significant alterations in GCL protein were observed.

GSH Concentration and Redox Status in Human NAFLD. GSH and GSSG concentrations were determined fluorometrically using the BioVision Glutathione Assay Kit (Mountain View, CA). The results are presented in Figure 5, along with the GSH:GSSG ratio (redox status). There were decreasing trends in GSH and GSSG concentrations throughout disease progression. The redox status (GSH:GSSG ratio), an estimation of the oxidative state in cells and tissues, is shown in Figure 5. The redox status exhibited a significant decreasing trend with disease progression.

MDA Concentration in Human NAFLD. Malondialdehyde (MDA) is a product of lipid peroxidation, and is often used as an indicator of oxidative stress in tissues and cells. MDA concentration was measured colorimetrically using the Cayman Chemical TBARS Assay Kit (Ann Arbor, MI). The results, shown in Figure 5 reveal a significant increasing trend in MDA concentration with disease progression.

Nrf2 Activation in Human NAFLD. Induction of ARE genes is dependent upon the escape of Nrf2 from Keap1-mediated degradation in the cytosol, enabling its translocation to the nucleus where it may bind to ARE promoters. In order to determine whether Nrf2 had translocated into the nuclei of hepatocytes and was therefore activated, formalin-fixed, paraffin-embedded human liver samples were immunohistochemically stained for Nrf2. Representative images are shown in Figure 6. Positive nuclear staining of Nrf2 (indicated by open arrows) can be seen in all stages of NAFLD. Nuclei negative for Nrf2 staining are indicated by closed arrows.

DMD Fast Forward. Published on August 30, 2010 as DOI: 10.1124/dmd.110.035006
This article has not been copyedited and formatted. The final version may differ from this version.

Quantification of Nrf2 translocation revealed that in normal human liver samples an average of 2.06% of hepatocytes within a 20X field of vision exhibited positive Nrf2 nuclear staining. In contrast, steatotic, NASH (fatty), and NASH (not fatty) samples presented on average with 24.67%, 22.60%, and 22.34% of hepatocytes bearing positive Nrf2 nuclear staining, respectively.

Discussion

NAFLD, like obesity, is becoming an increasingly significant health concern. Accumulation of triglycerides within hepatocytes, insulin resistance, inflammation, chronic oxidative stress levels, and fibrosis in combination, make this a complex disease. The specific mechanisms by which each of these parameters presents in the progression of NAFLD are not certain. With the exception of cytochrome P450 enzymes (Fisher *et al.*, 2009), the metabolic capacity towards administered pharmaceuticals in NAFLD patients has not been well characterized. This is of serious concern as NAFLD patients are often medicated for symptoms of the metabolic syndrome. Therefore, there is a great need for investigation into the pathogenic process of NAFLD as it relates to oxidative stress and the capacity to metabolize pharmaceuticals.

The aim of the current study was to investigate the expression and functionality of enzymes involved in the antioxidant response such as NQO1, GST, and GCL. Of these enzymes, the GST isoforms in particular, are known to play a significant role in the Phase II metabolism of endogenous molecules and administered pharmaceutical agents, while NQO1 is primarily responsible for the reduction of oxidative stress-inducing quinones. Increased expression and/or activity of NQO1 has been shown to be an important protective mechanism against oxidative stress in cholestasis (Aleksunes *et al.*, 2006b), coronary heart disease (Martin *et al.*, 2009), acetaminophen-induced hepatotoxicity (Moffit *et al.*, 2007), and primary biliary cirrhosis (Aleksunes *et al.*, 2006a). Though not traditionally considered a drug metabolizing enzyme, NQO1 is capable of reducing N-acetyl-p-benzo-quinone imine, the toxic quinone metabolite of acetaminophen (Moffit *et al.*, 2007). Furthermore, induction of NQO1 activity leads to protection against acetaminophen-induced hepatotoxicity (Moffit *et al.*, 2007). We have observed an increase in NQO1 mRNA levels, protein, and activity with the progression of NAFLD. These findings are similar to observations made in animal models of steatosis and NASH. We

previously found that Sprague-Dawley rats fed a methionine and choline-deficient (MCD) to induce NASH exhibited significant elevation of NQO1 mRNA and enzymatic activity (Lickteig *et al.*, 2007). In a separate study, rats fed the MCD diet exhibited significant induction of NQO1 mRNA levels, and when treated with oltipraz, an Nrf2 activator, were still able to induce NQO1 to an even greater level (Fisher *et al.*, 2008). Together with our previous animal studies, the current data suggest that as NAFLD progresses, increased NQO1 expression and activity levels may confer a greater capacity to protect NASH patients from oxidative stress-induced and pharmaceutical-induced quinone redox cycling.

Conversely, GSTs are responsible for protecting against electrophilic molecules such as those generated during oxidative stress or administration of pharmaceuticals. The expression and activity of specific GST isoforms has been closely associated with the severity of multiple diseases. For instance, GST M1 and T1 polymorphisms imparting an impairment of enzyme functionality impose a greater risk for coronary artery disease in Type II diabetes patients (Manfredi *et al.*, 2009). Furthermore, GST M1 functionality has been shown to be important in the protection against oxidative stress-induced DNA damage in maintenance hemodialysis patients (Lin *et al.*, 2009). Traditionally, the induction of GST isoforms has been associated with protective mechanisms due to their ability to catalyze the conjugation of GSH to various ROS molecules (Hayes *et al.*, 2005). Though several GST isoforms are inducible by Nrf2, there is generally a low, constitutive expression of GST A3, A4, M1, M3, and M4 (Aleksunes *et al.*, 2007), whereas GST A1 and A2 are believed to be more highly expressed in liver (Coles *et al.*, 2005). Moreover, GST A4 expression is believed to be induced during periods of prolonged oxidative stress (Coles *et al.*, 2005). GST P genes, on the other hand, are considered to be inducible, but not constitutively expressed within the liver (Henderson *et al.*, 2005). Presently, we have observed an increasing trend in GST A1, A2, A4, M3, and P1 mRNA expression throughout progression of NAFLD. The induction of GST P1 mRNA has previously been

recognized as a marker for hepatocellular carcinogenesis in the rat, but may or may not be associated with hepatocellular carcinoma in humans (Sakai *et al.*, 2007;Higashi *et al.*, 2004). Therefore, the induction of GST P1 shown presently may be an indicator of predisposition to hepatocellular carcinoma, but is not definitive. Presently, we have observed increases in GST A and P protein with disease progression. In contrast to GST A and P protein, there was a significant downward trend in GST M protein levels. These data suggest that the stability of each GST protein family may be differentially regulated throughout progression of NAFLD.

Due to the increased expression of multiple GST isoforms and induction of protein levels of the GST A and P families, GST enzymatic activity could be expected to similarly increase with the progression of NAFLD. However, in the current study, we observed a gradual decline in GST activity levels. These results suggest that as NAFLD advances, patients may have a reduced capacity to combat the oxidative insults of electrophilic compounds. A similar phenomenon has been observed in a murine model of ulcerative colitis (Clapper *et al.*, 1998). Interestingly, this downward trend in GST activity parallels the expression of GST M protein within our samples. GST A isoforms, on the other hand, are traditionally considered the dominant isoforms expressed in the liver (Coles *et al.*, 2005). These data indicate that there may be a more complicated mechanism of regulating GST isoforms during NAFLD progression.

Studies in human hepatic cirrhosis and hepatocellular carcinoma tissues have presented a complex interplay in GSH-dependent enzyme activities. These studies have shown that GST activity is significantly increased in cirrhotic livers compared to that of malignant hepatic tissue (Czeczot *et al.*, 2006). Further analysis in this study identified a significant reduction in GSH within cirrhotic hepatic tissue compared to both malignant and normal tissues (Czeczot *et al.*, 2006). In the current study, we observed a similar reduction in hepatic GSH levels during disease progression; and, though GSSG levels exhibited a significant downward trend, GSSG

concentrations were much higher than GSH. While this can sometimes be due to insensitivity of the analytical method employed or the labile nature of GSH in tissues, previous reports indicate that GSSG levels may indeed be much higher than GSH in NAFLD (Pastore *et al.*, 2003). Using the GSH and GSSG concentrations measured in each sample, we calculated the GSH:GSSG redox ratio which is an indicator of oxidative stress within the tissue. The reduction in GSH:GSSG redox ratio observed during NAFLD progression indicates that oxidative stress is increasing with the severity of disease. An additional indication of the presence of oxidative stress during NAFLD progression was observed by the increasing concentration of MDA with disease severity. MDA is a product of lipid peroxidation that occurs under oxidative stress conditions. Increasing levels of MDA confirm the conclusion of increased oxidative stress occurring during NAFLD made during the measurement of GSH levels. Nevertheless, the decrease in GST activity seen with NAFLD progression cannot be simply attributed to the measured reductions in GSH concentration. In this activity assay, GSH is supplemented in the reaction, thereby reducing the confounding effect of depletion of GSH pools in the sample. Therefore, this leads to the conclusion that additional factors must play a role in the conjugating capabilities of GST isoforms during NAFLD progression. One possible explanation is the adduction of 4-hydroxy-2-nonenal (HNE) to specific GST isoforms. Studies have identified GST P as a target of HNE adduction in human colorectal carcinoma cells (Codreanu *et al.*, 2009). Inhibition studies of GST P1 have indicated that cysteine 47, which is associated with the active site of the enzyme, is the target of covalent binding by HNE (van Iersel *et al.*, 1997). In the present study, we have observed a significant increase in expression of GST P protein which if inhibited by HNE may, in conjunction with GST M protein expression, explain the observed depletion in GST enzymatic activity. Further investigations are necessary to identify the specific mechanism by which GST activity is inhibited in NAFLD.

To identify whether the observed reductions in GSH concentration are due to a depletion of GSH pools or impairment of GSH synthesis, we investigated expression of the catalytic (GCLC) and modifying (GCLM) subunits of GCL. GCL is responsible for the initial catalysis of glutamate and cysteine to produce γ-glutamyl-l-cysteine (Lu, 2008). Further conjugation with glycine is catalyzed by GSH synthetase (Lu, 2008). GCL is regulated by feedback inhibition through GSH concentration, and induction of GCL expression does correlate with increased GSH synthesis; however, induction of GSH synthetase does not lead to a subsequent increase in GSH levels (Lu, 2008). In the current study, we have identified an increasing trend in GCLM mRNA levels; however, there was no significant alteration of GCLM protein levels. Additionally, no alterations to GCLC expression were observed. Together, these data provide no indication of an impairment of GSH synthesis, thereby leading to the conclusion that the observed reductions in GSH levels are most likely due to a depletion of GSH pools.

As stated previously, activation of the transcription factor Nrf2 leads to nuclear accumulation of Nrf2 protein and induction of downstream target ARE genes (Zhang, 2006). Currently, we have identified nuclear accumulation of Nrf2 in each of the stages of NAFLD. Quantification of hepatocytes exhibiting positive Nrf2 nuclear staining revealed a stark increase of the percentage of total hepatocytes in which Nrf2 was activated among each of the disease states compared to normal. Activation of Nrf2 is a viable explanation for the observed induction of ARE target genes. The increase in enzymatic activity of NQO1 implies an enhanced ability to diminish oxidative damage due to quinone redox cycling in NAFLD. However, the observed decrease in GST enzymatic activity suggests that NAFLD patients have a limited capacity to manage electrophilic compounds. The current study provides novel insight to the mechanisms of oxidative stress as they occur in the progression of human NAFLD.

Acknowledgements.

We would like to thank the NIH-funded Liver Tissue Cell Distribution System for continued assistance and procurement of liver tissue samples from patients with various stages of NAFLD. We also extend sincere appreciation to Marion Namenwirth (University of Minnesota), Melissa Thompson (Virginia Commonwealth University), and Dr. Stephen C. Strom and Kenneth Dorko (University of Pittsburgh).

References

Adams, L. A., and Lindor, K. D. (2007). Nonalcoholic Fatty Liver Disease. *Annals of Epidemiology* **17**, 863-869.

Aleksunes, L. M., Goedken, M., and Manautou, J. E. (2006a). Up-regulation of NAD(P)H:quinone oxidoreductase 1 during human liver injury. *World Journal of Gastroenterology* **12**, 1937-1940.

Aleksunes, L. M., and Manautou, J. E. (2007). Emerging Role of Nrf2 in Protecting Against Hepatic and Gastrointestinal Disease. *Toxicologic Pathology* **35**, 459-473.

Aleksunes, L. M., Slitt, A. L., Maher, J. M., Dieter, M. Z., Knight, T. R., Goedken, M., Cherrington, N. J., Chan, J. Y., Klaassen, C. D., and Manautou, J. E. (2006b). Nuclear factor-E2-related factor 2 expression in liver is critical for induction of NAD(P)H:quinone oxidoreductase 1 during cholestasis. *Cell Stress Chaperones* **11**, 356-363.

Ali, R., and Cusi, K. (2009). New diagnostic and treatment approaches in non-alcoholic fatty liver disease (NAFLD). *Annals of Medicine* **41**, 265-278.

Angulo, P. (2002). Nonalcoholic Fatty Liver Disease. *New England Journal of Medicine* **346**, 1221-1231.

Clapper, M. L., and Szarka, C. E. (1998). Glutathione S-transferase--biomarkers of cancer risk and chemopreventive response. *Chemico-Biological Interactions* **111-112**, 377-388.

Codreanu, S. G., Zhang, B., Sobecki, S. M., Billheimer, D. D., and Liebler, D. C. (2009). Global Analysis of Protein Damage by the Lipid Electrophile 4-Hydroxy-2-nonenal. *Molecular & Cellular Proteomics* **8**, 670-680.

Coles, B. F., and Kadlubar, F. F. (2005). Human Alpha Class Glutathione S-Transferases: Genetic Polymorphism, Expression, and Susceptibility to Disease. *Methods in Enzymology* **401**, 9-42.

Czeczot, H., Scibior, D., Skrzycki, M., and Podsiad, M. (2006). Glutathione and GSH-dependent enzymes in patients with liver cirrhosis and hepatocellular carcinoma. *Acta Biochimica Polonica* **53**, 237-241.

Fisher, C. D., Jackson, J. J., Lickteig, A. J., Augustine, L. M., and Cherrington, N. J. (2008). Drug metabolism enzyme induction pathways in experimental non-alcoholic steatohepatitis. *Archives of Toxicology* **82**, 959-964.

Fisher, C. D., Lickteig, A. J., Augustine, L. M., Ranger-Moore, J., Jackson, J. P., Ferguson, S. S., and Cherrington, N. J. (2009). Hepatic cytochrome P450 enzyme alterations in humans with progressive stages of nonalcoholic fatty liver disease. *Drug Metabolism and Disposition* **37**, 2087-2094.

Hayes, J. D., Flanagan, J. U., and Jowsey, I. R. (2005). Glutathione Transferases. *Annual Review of Pharmacology & Toxicology* **45**, 51-88.

Henderson, C. J., and Wolf, C. R. (2005). Disruption of the Glutathione Transferase Pi Class Genes. *Methods in Enzymology* **401**, 116-135.

Higashi, K., Hiai, H., Higashi, T., and Muramatsu, M. (2004). Regulatory mechanism of glutathione S-transferase P-form during chemical hepatocarcinogenesis: old wine in a new bottle. *Cancer Letters* **209**, 155-163.

Itoh, K., Chiba, T., Takahashi, S., Ishii, T., Igarashi, K., Katoh, Y., Oyake, T., Hayashi, N., Satoh, K., Hatayama, I., Yamamoto, M., and Nabeshima, Y. (1997). An Nrf2/Small Maf Heterodimer Mediates the Induction of Phase II Detoxifying Enzyme Genes Through Antioxidant Response Elements. *Biochemical and Biophysical Research Communications* **236**, 313-322.

Jaiswal, A. K. (2000). Regulation of Genes Encoding NAD(P)H:Quinone Oxidoreductases. *Free Radical Biology & Medicine* **29**, 254-262.

Jaiswal, A. K. (2004). Nrf2 Signaling in Coordinated Activation of Antioxidant Gene Expression. *Free Radical Biology & Medicine* **36**, 1199-1207.

Kleiner, D. E., Brunt, E. M., Van Natta, M., Behling, C., Contos, M. J., Cummings, O. W., Ferrell, L. D., Liu, Y., Torbenson, M. S., Unalp-Arida, A., Yeh, M., McCullough, A. J., and Sanyal, A. J. (2005). Design and Validation of a Histological Scroing System for Nonalcoholic Fatty Liver Disease. *Hepatology* **41**, 1313-1321.

Lickteig, A. J., Fisher, C. D., Augustine, L. M., and Cherrington, N. J. (2007). Genes of the Antioxidant Response Undergo Upregulation in a Todent Model of Nonalcoholic Steatohepatitis. *Journal of Biochemistry & Molecular Toxicology* **21**, 216-220.

Lin, Y. S., Hung, S. C., Wei, Y. H., and Tarng, D. C. (2009). GST M1 polymorphism associates with DNA oxidative damage and mortality among hemodialysis patients. *Journal of the American Society of Nephrology* **20**, 405-415.

Lu, S. C. (2008). Regulation of glutathione synthesis. *Molecular Aspects of Medicine* **30**, 42-59.

Manfredi, S., Calvi, D., del Fiandra, M., Botto, N., Biagini, A., and Andreassi, M. G. (2009). Glutathione S-transferase T1- and M1-null genotypes and coronary artery disease risk in patients with Type 2 diabetes mellitus. *Pharmacogenomics* **10**, 29-34.

Mannervik B, and Jemth P (1999) *Current Protocols in Toxicology*. 6.4.1-6.4.10. John Wiley & Sons, Inc., New York, Chichester, Weinheim, Brisbane, Singapore, Toronto.

Marra, F., Gastaldelli, A., Baroni, G. S., Tell, G., and Tiribelli, C. (2008). Molecular basis and mechanisms of progression of non-alcoholic steatohepatitis. *Trends in Molecular Medicine* **14**, 72-81.

Martin, N. J., Collier, A. C., Bowen, L. D., Pristsos, K. L., Goodrich, G. G., Arger, K., Cutter, G., and Pritsos, C. A. (2009). Polymorphisms in the NQO1, GSTT and GSTM genes are associated with coronary heart disease and biomarkers of oxidative stress. *Mutation Research* **674**, 93-100.

McCullough, A. J. (2006). Pathophysiology of Nonalcoholic Steatohepatitis. *Journal of Clinical Gastroenterology* **40**, S17-S29.

Moffit, J. S., Aleksunes, L. M., Kardas, M. J., Slitt, A. L., Klaassen, C. D., and Manautou, J. E. (2007). Role of NAD(P)H:quinone oxidoreductase 1 in clofibrate-mediated hepatoprotection from acetaminphen. *Toxicology* **230**, 197-206.

Nagata, K., Suzuki, H., and Sakaguchi, S. (2007). Common Pathogenic Mechanism in Development Progression of Liver Injury Caused by Non-Alcoholic or Alcoholic Steatohepatitis. *The Journal of Toxicological Sciences* **32**, 453-468.

Nakata, K., Tanaka, Y., Nakano, T., Adachi, T., Tanaka, H., Kaminuma, T., and Ishikawa, T. (2006). Nuclear REceptor-Mediated Transcriptional Regulation in Phase I, II, and III Xenobiotic Metabolizing Systems. *Drug Metabolism & Pharmacokinetics* **21**, 437-457.

Nguyen, T., Huang, H. C., and Pickett, C. B. (2000). Transcriptional Regulation of the Antioxidant Response Element. *Journal of Biological Chemistry* **275**, 15466-15473.

Pastore, A., Federici, G., Bertini, E., and Piemonte, F. (2003). Analysis of glutathione: implication in redox and detoxification. *Clinica Chimica Acta* **333**, 19-39.

Ross, D., and Siegel, D. (2004). NAD(P)H::Quinone Oxidoreductase 1 (NQO1, DT_Diaphorase), Functions and Pharmacogenetics. *Methods in Enzymology* **382**, 115-144.

Sakai, M., and Muramatsu, M. (2007). Regulation of glutathione transferase P: A tumor marker of hepatocarcinogenesis. *Biochemical and Biophysical Research Communications* **357**, 575-578.

Talalay, P., and Dinkova-Kostova, A. T. (2004). Role of Nicotinamide Quinone Oxidoreductase 1 (NQO1) in Protection against Toxicity of Electrophiles and Reactive Oxygen Intermediates. *Methods in Enzymology* **382**, 355-364.

van Iersel, M. L. P. S., Ploemen, J. H. T. M., Lo Bello, M., Federici, G., and van Bladeren, P. J. (1997). Interactions of α, β-unsaturated aldehydes and ketones with human glutathione *S*-transferase P1-1. *Chemico-Biological Interactions* **108**, 67-78.

Zhang, D. D. (2006). Mechanistic Studies of the Nrf2-KEAP1 Signaling Pathway. *Drug Metabolism Reviews* **38**, 769-789.

Footnotes

This work was supported by National Institutes of Health grants [DK068039], [ES006694] and [AT002842]. The Liver Tissue Cell Distribution System was sponsored by National Institutes of Health Contract [N01-DK-7-0004 / HHSN267200700004C].

Address correspondence to: Nathan Cherrington, Ph.D., Department of Pharmacology and Toxicology, College of Pharmacy, University of Arizona, 1703 East Mabel, Tucson, AZ 85721, Email: cherrington@pharmacy.arizona.edu

Figure Legends

Figure 1. Human NAFLD Histology. Representative hematoxylin and eosin staining of human liver samples diagnosed as normal, steatotic, NASH (fatty) and NASH (not fatty) are shown at 20X magnification. Steatosis was diagnosed as >10% fatty infiltration, NASH (fatty) as >5% fatty infiltration with significant inflammation and fibrosis, and NASH (not fatty) as <5% fatty infiltration with greater inflammation and fibrosis.

Figure 2. NAD(P)H:Quinone Oxidoreductase 1 (NQO1) Expression and Activity. Messenger RNA levels, densitometric analysis of NQO1 protein levels, and NQO1 enzymatic activity (2A) in human liver samples staged as normal, steatotic, NASH (fatty) and NASH (not fatty). mRNA levels were measured by the bDNA assay and expressed as relative light units (RLU) per 10 µg total RNA. Protein levels were determined by immunoblot analysis and expressed as relative to control protein (Total ERK). A representative blot of NQO1 and Total ERK is shown using two samples from each diagnostic category (2B). NQO1 activity was measured by the colorimetric reduction of DCPIP and expressed as nmol DCPIP reduced/minute/mg protein. Arrows indicate an increasing or decreasing trend and asterisks (*****) indicate a statistically significant trend as determined by non-parametric trend analysis ($p \leq 0.05$).

Figure 3. Glutathione S-Transferase (GST) Isoform Expression and Activity. Messenger RNA, densitometric analysis of protein levels of GST isoforms, and pan-GST enzymatic activity (3A, 3B, and 3D, respectively) in human liver samples diagnosed as normal, steatotic, NASH (fatty) and NASH (not fatty). mRNA levels (3A) for specific GST isoforms (GST A1, A2, A4, M1, M2, M3, M4, and P1) were measured by qPCR and expressed as relative mRNA expression to GAPDH. Protein levels (3B) of GST families (GSTA, GSTM, and GSTP) were determined by immunoblot analysis and expressed as relative to control protein (Total ERK). A representative

immunoblot of GSTA, GSTM and GSTP monomer and di\mer with Total ERK is shown (3C) using two samples from each diagnostic category. GST activity (3D) was determined spectrophotometrically using CDNB as a pan-GST substrate and expressed as µmol/minute/mg protein. Arrows indicate an increasing or decreasing trend and asterisks (*****) indicate a statistically significant trend as determined by non-parametric trend analysis ($p \leq 0.05$).

Figure 4. Glutamate Cysteine Ligase Catalytic (GCLC) and Modifying (GCLM) Subunit Expression. Messenger RNA (4A) and densitometric analysis of protein levels (4B) of GCLC and GCLM in human liver samples staged as normal, steatotic, NASH (fatty) and NASH (not fatty). mRNA levels were measured by the bDNA assay and expressed as relative light units (RLU) per 10 µg total RNA. Protein levels were determined by immunoblot analysis and expressed as relative to control protein (Total ERK). Arrows indicate an increasing or decreasing trend and asterisks (*****) indicate a statistically significant trend as determined by non-parametric trend analysis ($p \leq 0.05$).

Figure 5. Reduced (GSH) and Oxidized (GSSG) Glutathione Concentrations, Redox Status, and MDA Concentration. GSH, GSSG, and MDA concentrations in human liver samples diagnosed as normal, steatotic, NASH (fatty) and NASH (not fatty). GSH and GSSG concentrations were determined fluorometrically using o-phthalaldehyde as the probe, normalized to weight of tissue, and expressed as mM concentration. GSH and GSSG concentrations were then used to determine redox status of the tissue, and represented as the GSH:GSSG ratio. MDA concentrations were measured colorimetrically, concentrations determined by standard curve analysis, and expressed as µM concentration. Arrows indicate an increasing or decreasing trend and asterisks (*****) indicate a statistically significant trend as determined by non-parametric trend analysis ($p \leq 0.05$).

Figure 6. Immunohistochemical Staining of Nrf2. Representative immunohistochemical staining of Nrf2 in human liver samples staged as normal, steatotic, NASH (fatty) and NASH (not fatty). Antibody binding was detected by the avidin-biotin complex method using DAB for color development. Images are shown at 20X. Open arrows indicate nuclei positive for Nrf2 staining, and closed arrows indicate negative nuclear staining.

Figure 1

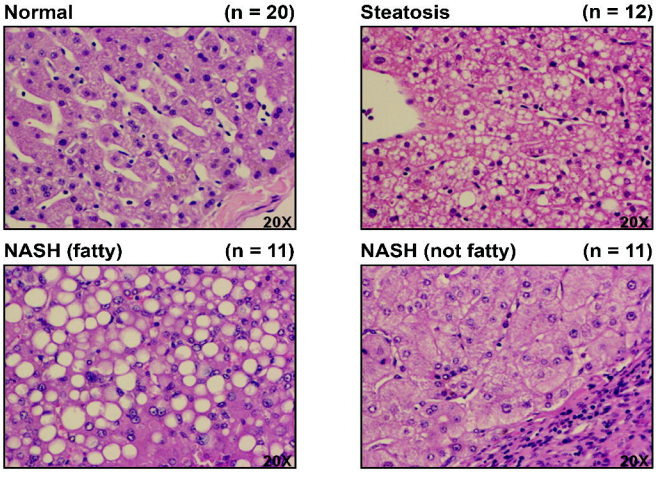
Normal
(n = 20)
20X
Steatosis
(n = 12)
20X
NASH (fatty)
(n = 11)
20X
NASH (not fatty)
(n = 11)
20X

Figure 2A

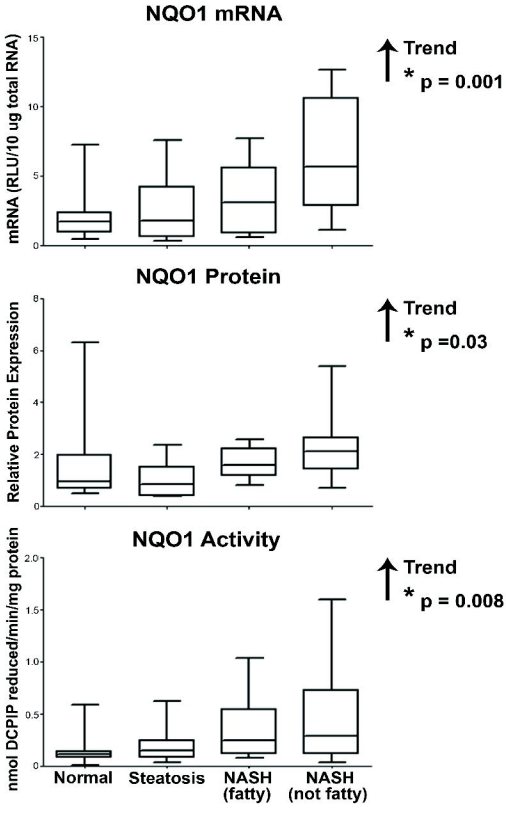

Figure 2B

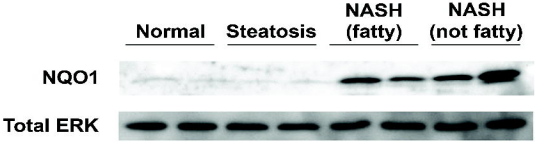

Figure 3A

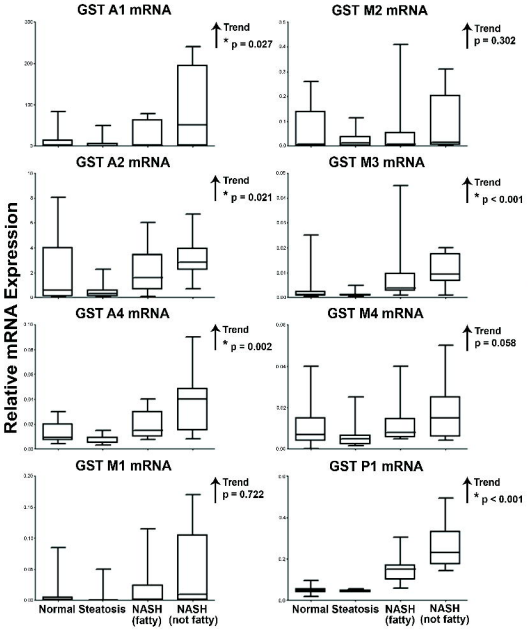

Figure 3B

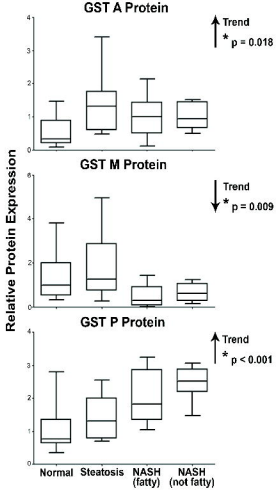

Figure 3C

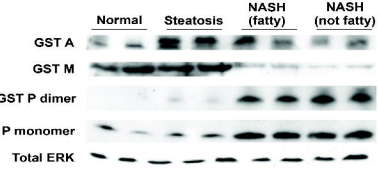

Figure 3D

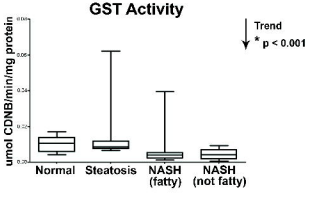

Figure 4A

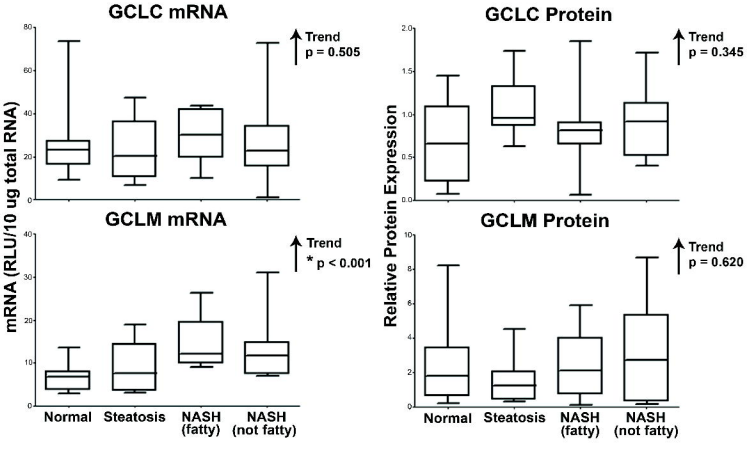

Figure 4B

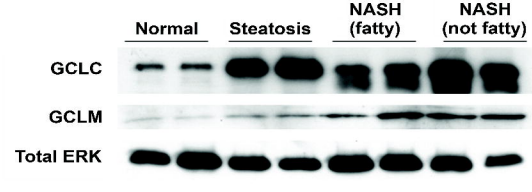

Figure 5

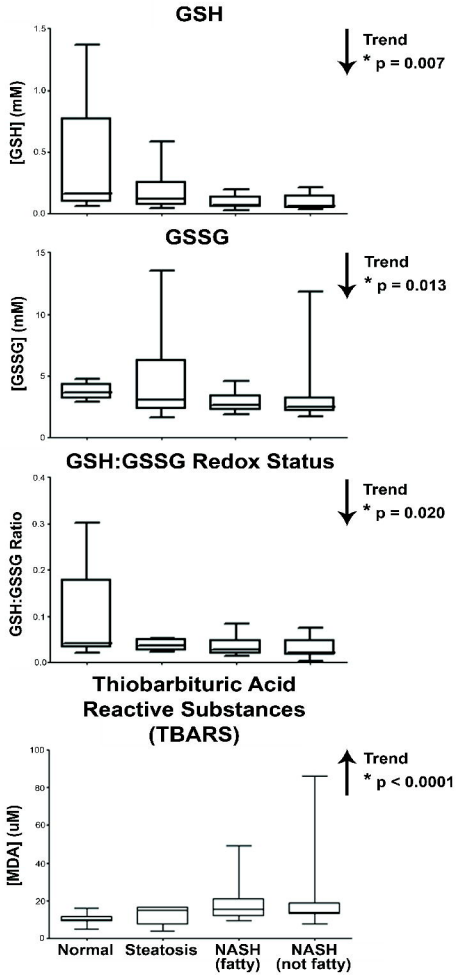
GSH
[GSH] (mM)
Trend
* p = 0.007
GSSG
[GSSG] (mM)
Trend
* p = 0.013
GSH:GSSG Redox Status
GSH:GSSG Ratio
Trend
* p = 0.020
Thiobarbituric Acid Reactive Substances (TBARS)
[MDA] (uM)
Trend
* p < 0.0001
Normal
Steatosis
NASH (fatty)
NASH (not fatty)

Figure 6

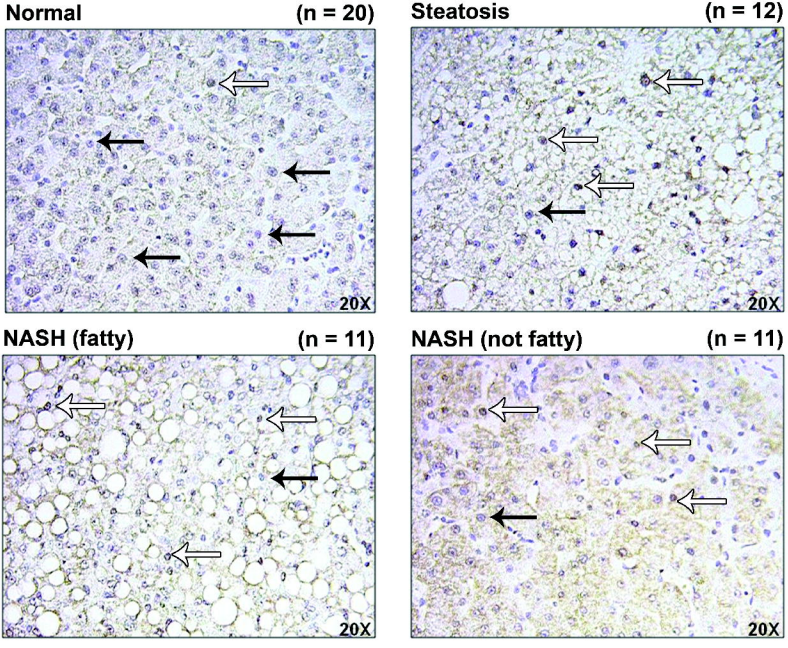

Diagnosis	Average Positive Hepatocyte Nuclei	Average Negative Hepatocyte Nuclei	Average Total Hepatocyte Nuclei	Average Percent Positive Nuclei
Normal	5.90	277.70	283.40	2.06
Steatosis	36.30	113.70	150.00	24.67
NASH (fatty)	22.05	80.55	102.95	22.60
NASH (not fatty)	25.65	92.85	113.10	22.34

DIVERSITY IN ANTIOXIDANT RESPONSE ENZYMES IN PROGRESSIVE STAGES OF HUMAN NON-ALCOHOLIC FATTY LIVER DISEASE

Rhiannon N. Hardwick, Craig D. Fisher, Mark J. Canet, April D. Lake, Nathan J. Cherrington

Department of Pharmacology and Toxicology, University of Arizona, Tucson AZ, USA

Supplemental Data Table 1.

Human Oligonucleotide Probe Sets.

Gene	Function	Probe Sequence
NQO1	CE	cagatggccttctttataagccaTTTTTctcttggaaagaaagt
	CE	gcggcttccagcttcttttgTTTTTctcttggaaagaaagt
	CE	ccagcctttcagaatggcagTTTTTctcttggaaagaaagt
	CE	tggagtgtgcccaatgctatatTTTTTctcttggaaagaaagt
	LE	aagttcgcagggtccttcagtTTTTTaggcataggacccgtgtct
	LE	gaacagactcggcaggatactgaTTTTTaggcataggacccgtgtct
	LE	ttcagccacaatatctgggctTTTTTaggcataggacccgtgtct
	LE	ggactccaaaccactgcaggTTTTTaggcataggacccgtgtct
	LE	tctcctatgaacactcgctcaaaTTTTTaggcataggacccgtgtct
	LE	acattcatgtccccgtggatTTTTTaggcataggacccgtgtct
	LE	ttgaattcgggcgtctgcTTTTTaggcataggacccgtgtct
	LE	gtttcttccatccttccaggatTTTTTaggcataggacccgtgtct
	LE	tcatcccaaatattctccaggcTTTTTaggcataggacccgtgtct
	BL	gggaactggaatatcacaaggtct
	BL	ggcagcgtaagtgtaagcaaac
	BL	cggaagggtcctttgtcatacat
	BL	tggaaagcactgccttcttactc

	BL	ccactgccaccagtggtga
	BL	cccttgcagagagtacatggag
	BL	cactctgaattggccagagaatg
	BL	agccacagaaatgcagaatgc
	BL	gtcagttgaggttctaagacttgga
GCLC	CE	tctgcagcgagctccgtgTTTTTctcttggaaagaaagt
	CE	agttctccagatgctctcttcttaaTTTTTctcttggaaagaaagt
	CE	tttactttcctaaatgctgatccaTTTTTctcttggaaagaaagt
	CE	gcatttttctttctgtagaatgtctagttTTTTTctcttggaaagaaagt
	LE	caaccatccaccactgcattgTTTTTaggcataggacccgtgtct
	LE	ctgttctgggccttgccaTTTTTaggcataggacccgtgtct
	LE	tctatgctcatgagggtgtactccTTTTTaggcataggacccgtgtct
	LE	tccttcccattgatgatggtgTTTTTaggcataggacccgtgtct
	LE	tggtgtccacatccacttccatTTTTTaggcataggacccgtgtct
	LE	ttagctttaggtagttcagaatactacatcTTTTTaggcataggacccgtgtct
	LE	catccatctggcaactgtcattTTTTTaggcataggacccgtgtct
	LE	gatggtttgcgataaactccctTTTTTaggcataggacccgtgtct
	LE	catttgcaatttggttacacttcaTTTTTaggcataggacccgtgtct
	LE	agtaactctgggcattcacataattTTTTTaggcataggacccgtgtct
	LE	ggatgagtcagttttacttccactatatTTTTTaggcataggacccgtgtct
	LE	ggtactgtagccagttcgtcaataatTTTTTaggcataggacccgtgtct
	LE	gggctggctgagaggcatTTTTTaggcataggacccgtgtct
	BL	ggatcagtccaggaaacacacct
	BL	gttttcaaggtaagagttcagaattg
	BL	tatgacactgtcttgcttgtagtcag

	BL	aaataaggctataattcatttcatcagt
GCLM	CE	aagagcttcttggaaacttgcttTTTTTctcttggaaagaaagt
	CE	aaatgtagccttttgatttgataattTTTTTctcttggaaagaaagt
	CE	caattttctctcatattgaaggaaattaTTTTTctcttggaaagaaagt
	LE	gaatgtcaggaatgctttcctgTTTTTaggcataggacccgtgtct
	LE	gcacccactcgtgcgcttTTTTTaggcataggacccgtgtct
	LE	accgcagtagccacagcgTTTTTaggcataggacccgtgtct
	LE	cctctacttttcacaatgaccgaatTTTTTaggcataggacccgtgtct
	LE	caggcagtaactagatttttacacatctTTTTTaggcataggacccgtgtct
	LE	atctgcctcaatgacaccatttaTTTTTaggcataggacccgtgtct
	BL	aagaacccctttcttttagcttgta
	BL	caggtaagttatgctcctaagtcagtt

Supplemental Data Table 2.

Human qPCR Primers.

Gene	Accession Number	Primers	Probe
GST A1	NM 000463.2	Forward: tatctccagcttccctctgc	64
		Reverse: gcttcttctaaagatttctcatcca	
GST A2	NM 000846.3	Forward: tttccagcttccctctgct	64
		Reverse: tgattcttctaaagatttctcatcca	
GST A4	NM 001512.3	Forward: agttgtacaagttgcaggatgg	62

		Reverse: caatttcaaccatgggcact	
GST M1	NM 000561.2	Forward: gacttcatctcccgctttga	28
		Reverse: cccagacagccatcttga	
GST M2	NM 000848.2	Forward: ggacttcatctcccgatttg	28
		Reverse: tctttgtgaacacaggtcttgg	
GST M3	NM 000849.4	Forward: gtgggataaaggcccagact	31
		Reverse: gtcttagccttaacttggaaatgc	
GST M4	NM 000850.3	Forward: acttcatctcccgctttgag	28
		Reverse: cccttgtgtacagaggttttgg	
GST P1	NM 000852.2	Forward: tccctcatctacaccaactatgag	56
		Reverse: ggttcttgcctccctggtt	